NJC

Structure-controlled intramolecular charge transfer in asymmetrically pyrene-based luminogens: Synthesis, characterization and optical properties

Journal:	*New Journal of Chemistry*
Manuscript ID	NJ-ART-06-2022-002968.R1
Article Type:	Paper
Date Submitted by the Author:	13-Jul-2022

Complete List of Authors:	Yu, Ze-Dong; Shandong University of Technology, School of Chemical Engineering Cao, Jing-Yi; Shandong University of Technology, School of Chemical Engineering Li, Hua-Long; Shandong University of Technology, School of Chemical Engineering Yang, Guang ; Shandong University of Technology, School of Chemical Engineering Xue, Zeng-Min; Shandong University of Technology, School of Chemical Engineering Jiang, Lu; Shandong University of Technology, School of Chemical Engineering Yu, Jia-Ying ; Shandong University of Technology, School of Chemical Engineering Wang, Chuan-Zeng; Shandong University of Technology, School of Chemical Engineering Liu, Xiang-Yu; Kyushu University, Graduate School of Integrated Sciences for Global Society Redshaw, Carl; University of Hull, Department of Chemistry Yamato, Takehiko; Saga University, Department of Chemistry and Applied Chemistry

ARTICLE

Structure-controlled intramolecular charge transfer in asymmetric pyrene-based luminogens: Synthesis, characterization and optical properties

Received 00th January 20xx,
Accepted 00th January 20xx

DOI: 10.1039/x0xx00000x

Ze-Dong Yu,[a] Jing-Yi Cao,[a] Hua-Long Li,[a] Guang Yang,[a] Zeng-Min Xue,[a] Lu Jiang,[a] Jia-Ying Yu,[a] Chuan-Zeng Wang,*[a,b] Xiang-Yu Liu,[c] Carl Redshaw[d] and Takehiko Yamato*[b]

Full-color emitting materials have been widely studied driven by their promising potential application in fluorescence imaging and optoelectronic devices. In this paper, the synthesis and charactization of four asymmetric D-A type pyrene-based luminogens **2** is presented. The experimental results revealed that this type of pyrene derivative possesses tunable optical properties by introducing D/A groups at the 1-, 3-positions and k-region (5-position) of the pyrene core. Wide emission bands from deep blue (429 nm) to yellow (567 nm) were obtained in different solutions or states. Combined with the theoretical calculations, this work provides an efficient strategy to develop pyrene-based full-color photoelectric materials.

Introduction

Although many scientists tend to specialize in just one field, no matter which study one pursues, other areas will have to be utilized in order to fully understand the implications of certain trends and conditions at both the micro and macro levels. This is very true for the field of organic optoelectronic materials.[1-3] There are many influencing factors among the structure-function relationships, such as solvent effects, substituent effects and site-effects, and these can be used to adjust intramolecular charge transfers (ICT) and intermolecular interactions.[4]

In recent years, donor/acceptor-π-acceptor/donor (D/A-π-A/D) type organic materials have been utilized in organic photovoltaics (OPV) cells,[5-6] organic light-emitting diodes (OLEDs) [7-8] and organic field effect transistors (OFETs).[9] This interest is mainly attributed to the ability to tune the optical properties of molecules based on the ICT theory.[10-13] Generally speaking, there is an efficiency strategy to obtain full color emission materials by employing the D-A unit since these types of structures are beneficial in narrowing the band gap between the highest occupied molecular orbitals (HOMOs) and lowest unoccupied molecular orbitals (LUMOs).[14-18] However, to date, fully comprehending the structure-property relationship remains a valuable and challenging topic in materials science.

As a *peri*-fused polycyclic aromatic hydrocarbon (PAH), pyrene has been investigated comprehensively due to its advantages, such as excellent electron accepting nature, high thermal stability and multiple functionalization and derivatization sites.[19] Compared to the more established functionalization at the 1-, 3-, 6-, 8-positions (Scheme 1a, 1b),[20,21] chemical modification at the K-region (4-, 5-, 9-, 10-positions) is more difficult to achieve because of regio-selectivity and purification issues (Scheme 1c).[22-24] In this context, the construction of pyrene-based D-π-A systems is challenging but highly required. The Müllen group employed the concept of D-A substitutions to constructed two double D-π-A pyrene derivatives in the K-region at the pyrene core, and provided an efficient strategy to tune the optoelectronic properties.[25] Subsequently, a series of D-A pyrene derivatives with unusual properties, such as red-to-NIR or white-light emission, were synthesized by introducing D-A substitutions at the 2-, 7-positions (Scheme 1d).[12, 26-27] The significant contributions to the HOMO−1/LUMO+1 orbitals endow the systems with properties that make them promising candidates as full-color displays and emitters.[28] In recent years, controllable regioselective approaches to obtain dipolar functionalization at the K-region (5-, 9-positions) and active sites (1-, 3-positions) of pyrene have been presented (Scheme 1e).[29,30] Adjustable photophysical properties were displayed, which can be ascribed to the efficient intramolecular charge transfer.[31]

However, mono-, or multi- symmetrical substitution patterns accounted for the vast majority among the current work reported on D-A pyrene derivatives.[19,23,32] Thus, the synthesis of asymmetrical D-A pyrene-based emitting materials is still a challenging research given the high symmetry of active-sites at the

[a] School of Chemistry and Chemical Engineering, Shandong University of Technology, Zibo 255049, P. R. China. E-mail: 13639028944@163.com
[b] Department of Applied Chemistry, Faculty of Science and Engineering, Saga University Honjo-machi 1, Saga 840-8502 Japan. E-mail: yamatot@cc.saga-u.ac.jp
[c] Graduate School of Integrated Sciences for Global Society, Kyushu University, 744 Motooka, Nishi-ku, Fukuoka 819-0395, Japan
[d] Department of Chemistry, The University of Hull, Cottingham Road, Hull, Yorkshire HU6 7RX, UK
† Footnotes relating to the title and/or authors should appear here.
Electronic Supplementary Information (ESI) available: [details of any supplementary information available should be included here]. See DOI: 10.1039/x0xx00000x

pyrene core. For precisely this reason, the design and synthesis of asymmetric luminogens has become a hot topic in pyrene chemistry.[33] Niko and co-workers explored asymmetrically tetrasubstituted pyrenes with surprising photophysical properties and potential applications as environmentally responsive probes.[34] The design and synthesis of asymmetrically 1,3-disubstituted pyrene derivatives along the short axis provides a new synthetic strategy by employing a two-step bromination reaction.[35]

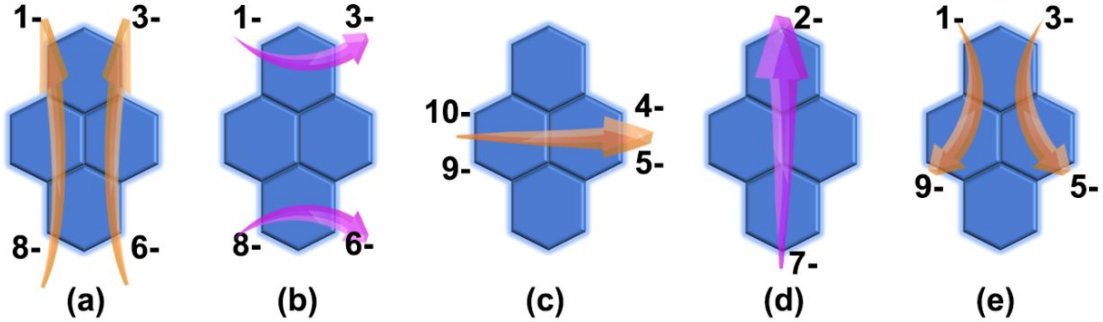

Scheme 1 Schematic representation of reported D-π-A type pyrene patterns.

Recently, two mechanochromic luminogens with intriguing emission behavior were synthesized by introducing D-A groups at the 1-, 3-positions and k-region (5-position) of the pyrene core.[36] Herein, the efficient strategy to construct asymmetric D-A type pyrene luminogens was further confirmed, and four asymmetrically D-A pyrenes **2** functionalized along the long axis were synthesized (Scheme 2). The optical properties of the luminogens **2** were systematic discussed and combined with theoretical calculations, the interesting structure-property relationships indicate that the mentioned methodologies have potential for the synthesis of full-color emitters.

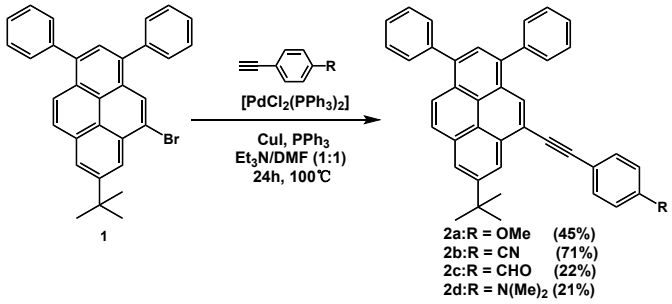

Scheme 2 Synthetic route to compounds **2**.

Results and discussion

Synthesis of luminogens 2a–d

The synthetic procedures for luminogens **2a-d** are shown in Scheme 2. Briefly, 7-*tert*-butyl-1, 3-diphenyl-5-substituted pyrenes were synthesized from 7-*tert*-butyl-1,3-diphenyl-5-bromopyrene **1**[30] as starting compound by a Sonogashira coupling reaction in reasonable yields. All compounds were fully characterized by $^{1}H/^{13}C$ NMR spectroscopy and high resolution mass spectrometry (Figures S1–8, ESI‡). As one of the few synthetic strategies for asymmetrical luminogens substituted at the 1-, 3-positions and k-region (5-position) of the pyrene core, their photophysical properties also further stimulated our research interest.

Photophysical properties

The UV absorption of luminogens **2** was recorded in dilute solutions and emission behavior was investigated in solution and in the solid state; the detailed parameters are present in Table 1. Specifically, the UV absorption spectra of these four luminogens **2a-d** in dilute CH_2Cl_2 is depicted in Fig. 1, and similar absorption bands with slightly red-shift from **2a** to **2d** were observed.

There are mainly two sets of strong absorption bands peaking in the 297–338 nm and 386–391 nm range. The high-energy absorption bands with a shoulder peak are assigned to the π-π* transition from the extended π system between the substituent aryl ethynyl/phenyl groups and the pyrene core. The low-energy absorption band centered at 386–391 nm with equivalent intensity compared to the that mentioned above, may be ascribed to the ICT transition from the aryl ethynyl moiety to the pyrene core.[31] To verify these results, further investigation of the absorption behavior was performed in different solvents (see Figures S9–S12 in the Supporting Information). A certain amount of red shift (2–9 nm) was observed for **2** on going from the nonpolar solvent cyclohexene to the polar solvent dimethylformamide (DMF), which indicates that ICT behavior exists in this D-A pyrene-based system.

Table 1 The photophysical properties of D-A pyrene-based luminogens **2**.

Comp.	λ_{abs} (nm) sol[a]	λ_{em} (nm) Sol[b]/solid	HOMO (eV)[c]	LUMO (eV)[c]	ΔE_g (eV)[c]	Φ_{FL}[d] Sol/solid
2a	297,320,388	434 / 492	-4.93	-1.72	3.21	0.76/0.06
2b	303,328,386	468 / 483	-5.29	-2.23	3.06	0.74/0.04
2c	304,328,389	509 / 519	-5.23	-2.25	2.98	0.39/0.02
2d	299,338,391	510 / 494	-4.69	-1.62	3.07	0.78/0.02

[a] 1×10^{-5} M in CH_2Cl_2, λ_{abs} is the absorption band appearing at room temperature.
[b] 1×10^{-7} M in CH_2Cl_2, λ_{ex} is the fluorescence band appearing at the shortest wavelength.
[c] DFT/B3LYP/6-31G* using Gaussian.
[d] Absolute quantum yield (± 0.01–0.03)

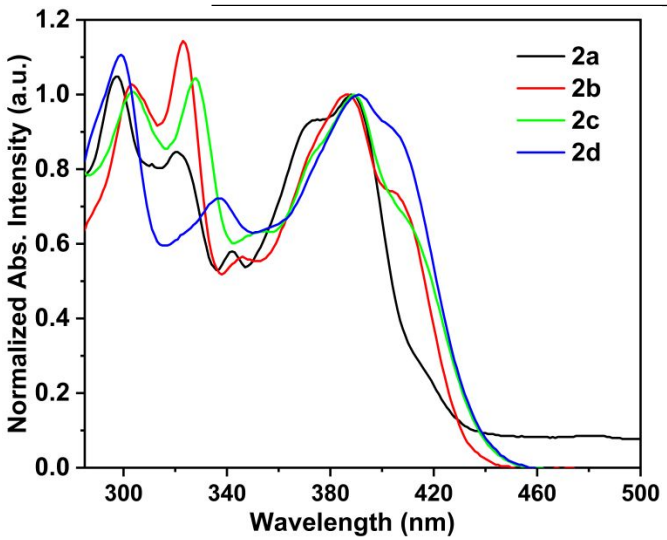

Fig. 1 Absorption spectra of **2a–d** in CH_2Cl_2 (spectrometric grade, concentration 1×10^{-5} M)

To aid in the interpretation of the structure-property relationships, the systematic emission properties of the luminogens **2** were studied in solution and in the solid state (see Fig. 2). As shown in Fig. 2A, the four luminogens **2** exhibited distinct emission properties, and a large red-shift (83 nm) was observed from **2a** to **2d**, which mainly was attributed to the gradual increased intramolecular charge transfer. More specifically, the difference of the *para* substituted moieties on the terminal phenyl plays an important role in adjusting the emission properties. In the 1,3-di-D-5-A asymmetric system, the *para* substituents either increase or decrease the electron-withdrawing ability of the phenylalkynyl group. As a weak electron-donating group, the methoxy group weakens the electron-withdrawing ability of the phenylalkynyl moiety, and results in weakened ICT behavior. Thus, compound **2a** exhibited almost monomer emission with maximum emission at 434 nm.[37] The ICT emission state plays a minor role in this dilute solution. In sharp contrast, in the other three luminogens, emission maxima centered at 468 nm for **2b**, 509 nm for **2c**, 510 nm for **2d**, and large red-shifts were observed benefiting from the strong electron-withdrawing groups (–CN, –CHO) and strong electron-donating group ($-N(CH_3)_2$). These results indicate that ICT emission states are formed for these monomers in dilute solution.[38,39] All emission behavior show that the asymmetric D-A type design strategy is highly efficient to tune the emission properties of pyrene-based materials in solution.

To evaluate the performance of the materials and interpret the emission behavior, analysis of the detailed solvatochromic effects in different organic solvents (cyclohexane, 1,4-dioxane, tetrahydrofuran (THF), dichloromethane (DCM) and dimethylformamide (DMF)) with various polarities and absolute fluorescence quantum yields (Φ_{FL}) was performed. As shown in Fig. 2C and Figures S13-S15, more obvious solvatochromic effects were observed for the emission spectra *versus* the absorption spectra. As mentioned above, compound **2a** displays a slight bathochromic-shift (about 6nm) on moving from cyclohexane to DMF, while significant red-shifts (50 nm for **2b**, 61 nm for **2c**, 131 nm for **2d**) were present. Taking **2d** as an example, the luminogens **2d** exhibited obvious color changes from deep blue in cyclohexane (CIE: x=0.14, y=0.07) to yellow in DMF (CIE: x=0.45, y=0.53); results are presented in Fig. 2D under a UV light (365 nm) as a inset. This further indicates that luminogens **2** are modifiable, tunable fluorescent materials. What's more, all compounds, except for **2c**, exhibit high quantum yields (greater than 70%). Because of the presence of the strong electron-withdrawing group (–CHO), compound **2c** presents low quantum yield (39%), which may be ascribe to the low electron transition probability. On the whole, these are exciting results for the D-π-A system with a noteworthy intramolecular charge transfer. Subsequently, the emission properties in the solid state were studied (see Fig. 2B). Interesting phenomena are present which different from the effects noted in diluted organic solutions. The maximum emission peaks for luminogens **2** centered at 483–519 nm are in the order **2b** < **2a** < **2d** < **2c**, inconsistent with the electronegativity of the *para* substituted moieties on the terminal phenyl. Meanwhile, the value of Φ_{FL} is lower than 10% in the solid state, which may be attributed to the intermolecular interactions in the aggregated state. Most likely, excimer emission plays a dominant role because of the π-π interactions and dimer overlap between adjacent molecules.

ARTICLE

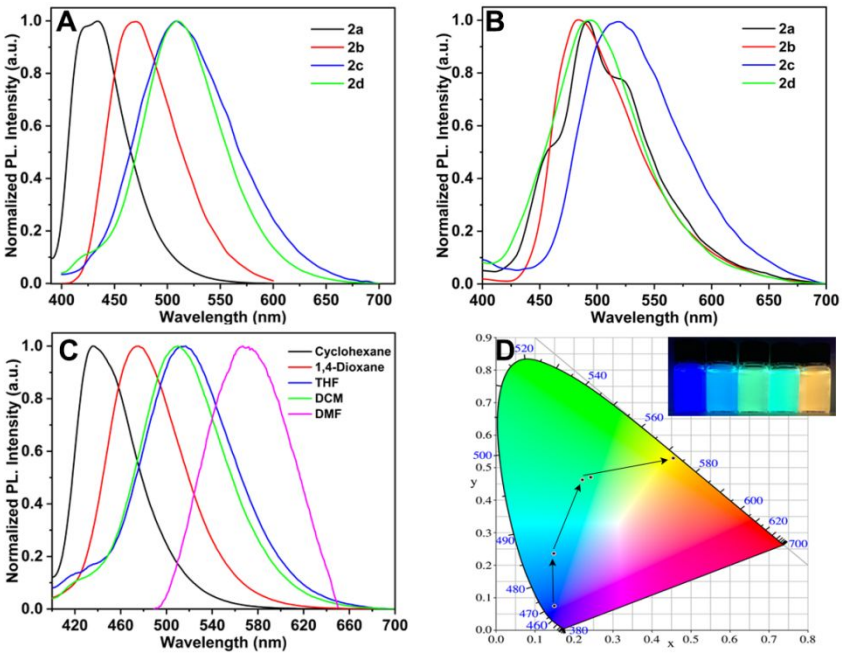

Fig. 2 Emission spectra of fluorophores **2** in CH_2Cl_2 solution (A) and in the solid state (B); solvatochromism effect of emission spectra (C) and CIE 1931 chromaticity diagram (D) for **2d**. (Inset: Fluorescent photographs of **2d** in cyclohexane, 1,4-dioxane, THF, DCM and DMF, respectively).

To illustrate this luminescence mechanism in diluted solution and in the solid state, the concentration effect was investigated in dichloromethane at room temperature. Taking **2a** for example, Fig. 3A shows the fluorescence emission spectra of compound **2a** at different concentrations from 5×10^{-8} M to 1×10^{-3} M. Clearly, on increasing the concentration, the emission intensity and maximum emission wavelength are also changed. Overall speaking, the emission peaks remain almost constant while the emission intensity was slightly increased within the concentration increases to 5×10^{-6} M, and when increased ten-fold to 5×10^{-5} M, the emission intensity increased sharply to the maximum with a significant red-shift. The emission intensity gradually decreased upon increasing the concentration from 5×10^{-5} M to 1×10^{-3} M, and is accompanied by a continuous red-shift up to 452 nm. Understandably, as shown in Fig. 3B, persistent red-shift (the point of blue star) was observed on account of the greater aggregation in the solid state on the basis of concentration effects.[40, 41] Compared to the emission behavior in dilute solution, the excimer emission plays a dominant role with the intensification of aggregation. Both **2b** and **2c** also present similar emission properties in line with the formation of molecular aggregates. However, **2d** displayed a marked difference for its maximum emission wavelength with obvious blue-shift in the solid state. This may be ascribed to the transformation of the packing arrangement and molecular configurations in the different states.[42]

ARTICLE

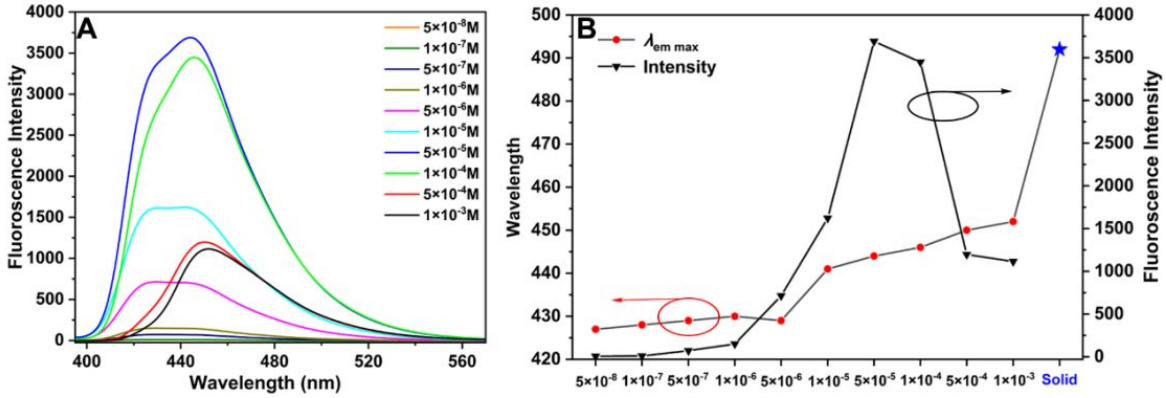

Fig. 3 A: Effect of concentration on the fluorescence emission spectra of **2a** recorded in DCM at room temperature; B: Plots of maximum emission wavelength (red circle) and emission intensity (black circle) in different concentrations.

Theoretical explorations were carried out in to verify the influence of the intramolecular charge transfer on the optical properties in this asymmetrical D-A system at the B3LYP/6-31g-(d) level.[43, 44] As expected, the *para* substituted moieties on the terminal phenyl basically determined the distributions of their lowest unoccupied molecular orbital (LUMO) and highest occupied molecular orbital (HOMO). As depicted in Fig. 4, the electron-donating/withdrawing substituents play a vital role to tune the HOMO-LUMO energy gap, and further to achieve structure-controlled synthetic strategy in asymmetrically pyrene-based materials. Specifically, the electron-donating groups (–OMe, –$N(CH_3)_2$) can provide an obvious contribution to HOMOs, on the other hand, the electron-withdrawing groups (–CN, –CHO) have a significant effect on the LUMOs, then tailored energy gap was obtained. Thus, the donating or withdrawing-electrons ability for the *para* substituted moieties influence the photophysical properties as the major cause.

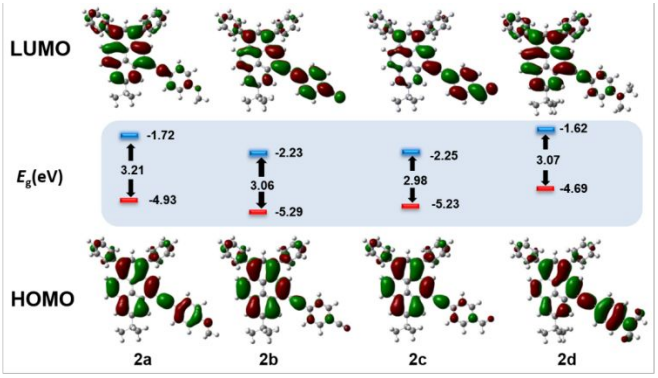

Fig. 4 Frontier-molecular-orbital distributions and energy levels diagram of **2** by DFT calculations.

Experimental

All reactions were carried out under a dry N_2 atmosphere. ^{1}H NMR (400 MHz) and ^{13}C NMR (100 MHz) spectra were recorded on a WJGS-037 Bruker AVANCE III 400 NMR spectrometer with $SiMe_4$ as an internal reference: *J*-values are given in Hz.

Materials

Solvents were Guaranteed reagent (GR) for cyclohexane, tetrahydrofuran (THF), dichloromethane (CH_2Cl_2), acetonitrile (CH_3CN), and dimethylformamide (DMF), and stored over molecular sieves. Unless otherwise stated, all other reagents were obtained commercially and used without further purification.

Synthetic procedures

Synthesis of 7-*tert*-butyl-1,3-diphenyl-5-bromopyrene (1)

The compound **1** was synthesized from 7-*tert*-butyl-1,3-diphenylpyrene with the corresponding equiv. of Br_2 in the presence of iron powder. The detailed synthetic steps have been reported in previous work.[30] ^{1}H-NMR spectrum of this precursor is fully consistent with the published spectra.

Synthesis of 7-*tert*-butyl-1,3-diphenyl-5-arylethynylpyrenes (2a–2d)

The series of compounds **2a–2d** were synthesized from **1** with the corresponding aryl alkyne by a Sonogashira coupling reaction.

Synthesis of 7-*tert*-butyl-1,3-diphenyl-5-(4'-methoxyphenyl-ethynyl)pyrene (2a)

A mixture of **1** (100 mg, 0.2 mmol), 4-methoxyphenylacetylene (40 mg, 0.3 mmol), $PdCl_2(PPh_3)_3$ (12 mg, 0.02 mmol), CuI (7.6 mg, 0.4 mmol), PPh_3 (8 mg, 0.03 mmol) were added to a degassed solution

of Et_3N (5 mL) and DMF (5 mL). The resulting mixture was stirred at 100 °C for 24 h. After it was cooled to room temperature, the reaction was quenched with water. The mixture was extracted with CH_2Cl_2 (2 × 50 mL), the organic layer was washed with water (2 × 30 mL) and brine (30 mL), and then the solution was dried with $MgSO_4$, and concentrated under reduced pressure. The residue was recrystallized from CH_2Cl_2: Hexane = 1:4 to give **2a** as a yellow solid (48.7 mg, 45%). M.p. 241–242 °C; ^{1}H NMR (400 MHz, $CDCl_3$): δ_H = 8.86 (s, 1H, pyrene-*H*), 8.47 (s, 1H, pyrene-*H*), 8.26 (s, 1H, pyrene-*H*), 8.18 (d, *J* = 9.2 Hz, 1H, pyrene-*H*), 8.04 (d, *J* = 9.2 Hz, 1H, pyrene-*H*), 7.95 (s, 1H, pyrene-*H*), 7.71 – 7.45 (m, 10H, Ar-*H*), 6.96 (d, *J* = 6.9 Hz, 2H, Ar-*H*), 6.86 (d, *J* = 6.9 Hz, 2H, Ar-*H*), 3.83 (d, *J* = 1.5 Hz, 3H, OMe), 1.64 (s, 9H, *t*Bu) ppm; ^{13}C NMR (100 MHz, $CDCl_3$) δ_C = 159.81, 149.51, 140.97, 140.84, 137.88, 137.32, 134.07, 133.19, 131.31, 130.74, 130.63, 129.40, 129.29, 128.54, 128.43, 127.87, 127.65, 127.43, 127.39, 127.14, 124.96, 124.92, 123.30, 122.96, 121.16, 120.76, 115.58, 114.21, 94.61, 87.14, 55.39, 35.44, 31.96 ppm; FAB-MS: m/z calcd for $C_{41}H_{32}O$ 540.2453 [M^+]; found 540.2449 [M^+].

A similar process using 4-cyanophenyl acetylene, 4-formylphenylacetylene, 4-*N*,*N*-dimethylphenyl acetylene, was followed for the synthesis of **2b**, **2c,** and **2d**, respectively.

7-*tert*-Butyl-1,3-diphenyl-5-(4′-cyanophenylethynyl)pyrene (**2b**) was obtained as a yellow floccule solid (The residue was purified by column chromatography eluting with a 1:2 CH_2Cl_2/Hexane mixture, 76.1 mg, 71%). M.p. 310–311 °C; ^{1}H NMR (400 MHz, $CDCl_3$) δ_H = ^{1}H NMR (400 MHz, $CDCl_3$) δ_H = 8.78 (s, 1H, pyrene-*H*), 8.53 (s, 1H, pyrene-H), 8.28 (s, 1H, pyrene-H), 8.19 (d, *J* = 9.3, 1H, pyrene-H), 8.05 (d, *J* = 9.3, 1H, pyrene-*H*), 7.97 (s, 1H, pyrene-*H*), 7.80–7.45 (m, 14H, Ar-*H*), 1.64 (s, 9H, *t*Bu) ppm; ^{13}C NMR (100 MHz, $CDCl_3$) δ_C = 148.66, 139.69, 139.53, 137.59, 136.70, 131.18, 131.05, 130.42, 130.34, 129.84, 129.64, 129.52, 128.89, 128.47, 128.32, 127.55, 127.42, 126.86, 126.63, 126.53, 126.49, 125.73, 124.22, 124.04, 122.19, 119.65, 118.30, 117.55, 110.50, 91.88, 91.65, 34.40, 30.88 ppm; FAB-MS: m/z calcd for $C_{41}H_{29}N$ 535.2301 [M^+]; found 535.2301 [M^+].

7-*tert*-Butyl-1,3-diphenyl-5-(4′-formylphenylethynyl)pyrene (**2c**) was obtained as an orange solid (recrystallized from Hexane: CH_2Cl_2 = 2:1, 24 mg, 22%). M.p. 278–280 °C; ^{1}H NMR (400 MHz, $CDCl_3$) δ_H = 10.04 (s, 1H, CHO-*H*), 8.82 (s, 1H, pyrene-*H*), 8.54 (s, 1H, pyrene-*H*), 8.28 (s, 1H, pyrene-*H*), 8.18 (d, *J* = 9.3, 1H, pyrene-*H*), 8.04 (d, *J* = 9.3, 1H, pyrene-*H*), 7.97 (s, 1H, pyrene-*H*), 7.91 (d, *J* = 8.1, 2H, Ar-*H*), 7.81 (d, *J* = 8.1, 2H, Ar-*H*), 7.68 (t, *J* = 8.3, 4H, Ar-*H*), 7.55 (m, 6H, Ar-*H*), 1.64 (s, 9H, *t*Bu) ppm; ^{13}C NMR (100 MHz, $CDCl_3$) δ_C = 191.45, 149.71, 140.80, 140.63, 138.55, 137.72, 135.48, 132.16, 131.39, 130.75, 130.72, 130.59, 130.04, 129.78, 129.52, 128.69, 128.61, 128.48, 127.92, 127.69, 127.58, 127.52, 126.86, 125.25, 125.07, 123.28, 123.22, 120.84, 119.64, 93.58, 92.61, 35.47, 31.95 ppm; FAB-MS: m/z calcd for $C_{41}H_{30}O$ 538.2297 [M^+]; found 538.2297 [M^+].

7-*tert*-Butyl-1,3-diphenyl-5-(4′-*N*,*N*-dimethylphenylethynyl)pyrene **2d** was obtained as a yellow solid (recrystallized from hexane:CH_2Cl_2 = 4:1, 23 mg, 21%). M.p. 240–241°C; ^{1}H NMR (400 MHz, $CDCl_3$) δ_H = 8.89 (s, 1H, pyrene-*H*), 8.45 (s, 1H, pyrene-*H*), 8.25 (s, 1H, pyrene-*H*), 8.16 (d, *J* = 9.3, 1H, pyrene-*H*), 8.03 (d, *J* = 9.3, 1H, pyrene-*H*), 7.94 (s, 1H, pyrene-*H*), 7.69 (m, 4H, Ar-*H*), 7.61–7.53 (m, 6H, Ar-*H*), 7.53–7.46 (m, 2H, Ar-*H*), 6.77–6.70 (m, 2H, Ar-*H*), 3.02 (s, 6H, Me), 1.64 (s, 9H, *t*Bu) ppm; ^{13}C NMR (100 MHz, $CDCl_3$) δ_C = 148.34, 139.99, 139.88, 136.51, 136.08, 131.82, 131.67, 130.25, 130.21, 129.69, 129.58, 129.38, 128.30, 127.51, 127.45, 127.34, 126.77, 126.56, 126.30, 126.27, 126.23, 123.83, 123.69, 122.24, 121.78, 120.26, 110.93, 94.97, 85.43, 39.23, 34.37, 30.91, 28.68 ppm; FAB-MS: m/z calcd for $C_{42}H_{35}N$ 553.2270 [M^+]; found 553.2270 [M^+].

Conclusions

In summary, four asymmetric D-A pyrene-based luminogens with tunable and excellent photophysical properties were designed and synthesized. Systematic investigation and evaluation based on the experimental measurements and theoretical calculations were performed. A series of multi-color luminescent materials with reasonable yield and stability were afforded by fine-tuning the *para* substituents at the terminal phenyl. High quantum yields in solutions (almost all are greater than 74%) suggests such compounds have promising application potential. Moreover, these results indicated that the construction of asymmetric D-A structures is an efficient and feasible strategy to achieve efficient full-color emission materials.

Conflicts of interest

There are no conflicts to declare.

Acknowledgements

This work was performed under the Cooperative Research Program of "Network Joint Research Center for Materials and Devices (Institute for Materials Chemistry and Engineering, Kyushu University)". We would like to thank the Natural Science Foundation of Shandong Province (Grant No. ZR2019BB067). This research used resources of the Advanced Light Source, which is a DOE Office of Science User Facility under contract no. DE-AC02-05CH11231. CR thanks the University of Hull for support.

Notes and references

‡ Footnotes relating to the main text should appear here. These might include comments relevant not central to the matter under discussion, limited experimental and spectral data, and crystallographic data.

1 H. Primas, Chemistry, Quantum Mechanics and Reductionism: Perspectives in Theoretical Chemistry. Berlin, Heidelberg: Springer Verlag, 1981.
2 M. Tepliakova, I. K. Yakushenko, E. I. Romadina, A. V. Novikov, P. M. Kuznetsov, K. J. Stevenson and P. A. Troshin, *Sustainable Energy Fuels*, 2021, **5**, 283–288.
3 J. Qiu, H. Liu, X. Li and S. Wang, *Chemical Engineering Journal*, 2020, **387**, 123965
4 Y. Yu, H. Xing, Z. Zhou, J. Liu, H. H.-Y. Sung, I. D. Williams, J. E. Haloert, Z. Zhao and B. Z. Tang, *Sci. China Chem.*, 2022, **65**, 135–144.
5 O. P. Lee, A. T. Yiu, P. M. Beaujuge, C. H. Woo, T. W. Holcombe, J. E. Millstone, J. D. Douglas, M. S. Chen and J. M. J. Fréchet, *Adv. Mater.*, 2011, **23**, 5359–5363.
6 C. Y. Wang, T. Okabe, G. Long, D. Kuzuhara, Y. Zhao, N. Aratani, H. Yamada and Q. C. Zhang, *Dyes Pigm.*, 2015, **122**, 231-237.

7 J. Jayabharathi, J. Anudeebhana, V. Thanikachalam and S. Sivaraj, *RSC Adv.*, 2020, **10**, 8866–8879.
8 L. Yao, S. T. Zhang, R. Wang, W. J. Li, F. Z. Shen, B. Yang, and Y. G. Ma, *Angew. Chem.*, 2014, **126**, 2151–2155.
9 P.-Y. Gu, J. Zhang, G. K. Long, Z. L. Wang and Q. C. Zhang, *J Mater. Chem. C*, 2016, **4**, 3809–3814.
10 Z. R. Grabowski, K. Rotkiewicz and W. Rettig, *Chem. Rev.*, 2003, **103**, 3899-4031.
11 R. Maitra, J.-H. Chen, C.-H. Hu and H. M. Lee, *Eur. J Org. Chem.*, 2017, **40**, 5975–5985.
12 J. Merz, J. Fink, A. Friedrich, I. Krummenacher, H. A. Mamari, S. Lorenzen, M. Hähnel, A. Eichhorn, M. Moos, M. Holzapfel, H. Braunschweig, C. Lambert, A. Steffen, L. Ji and T. B. Marder, *Chem. Eur. J*, 2017, **23**,13164–13180.
13 T. R. Hopper, D. P. Qian, L. Y. Yang, X. H. Wang, K. Zhou, R. Kumar, W. Ma, C. He, J.-H. Hou, F. Gao and A. A. Bakulin, *Chem. Mater.*, 2019, **31**, 6860–6869.
14 P. Das, A. Kumar, A. Chowdhury and P. S. Mukherjee, *ACS Omega*, 2018, **3**, 13757–13771.
15 M. Ahn, M.-J. Kim, D. W. Cho and K.-R. Wee, *J. Org. Chem.*, 2021, **86**, 403–413.
16 R. Flamholc, A. Wrona-Piotrowicz, A. Makal and J. Zakrzewskia, *Dyes Pigm.*, 2018, **154**, 52-61.
17 A. A. Kalinin, S. M. Sharipova, T. I. Burganov, A. I. Levitskaya, Y. B. Dudkina, A. R. Khamatgalimov, S. A. Katsyuba, Y. H. Budnikova and M. Yu. Balakina, *Dyes Pigm.*, 2018, **156**, 175–184.
18 M. Ahn, M.-J. Kim and K.-R. Wee, *J. Org. Chem.*, 2019, **84**, 12050–12057.
19 T. M. Figueira-Duarte and K. Müllen, *Chem. Rev.*, 2011, **111**, 7260–7314.
20 R. Zhang, Y. Zhao, T. Zhang, L. Xu and Z. Ni, *Dyes Pigm.*, 2016, **130**, 106–115.
21 R. Zhang, H. Sun, Y. Zhao, X. Tang and Z. Ni, *Dyes Pigm.*, 2018, **152**, 1–13.
22 K. Ozaki, K. Kawasumi, M. Shibata, H. Ito and K. Itami. *Nat. Commu.*, 2015, **6**, 6251.
23 X. Feng, J.-Y. Hu, C. Redshaw and T. Yamato, *Chem. Eur. J.*, 2016, **22**, 11898–11916.
24 F. Shahrokhi, R. F. Estabragh and Y. M. Zhao, *New J. Chem.*, 2020, **44**, 16786–16794.
25 L. Zöphel, V. Enkelmann and K. Müllen, *Org. Lett.*, 2013, **15**, 804–807.
26 L. Ji, R. M. Edkins, A. Lorbach, I. Krummenacher, C. Brückner, A. Eichhorn, H. Braunschweig, B. Engels, P. J. Low and T. B. Marder, *J. Am. Chem. Soc.*, 2015, **137**, 6750–6753.
27 X. Feng, C. Qi, H.-T. Feng, Z. Zhao, H. H. Y. Sung, I. D. Williams, R. T. K. Kwok, J. W. Y. Lam, A. Qin and B. Z. Tang, *Chem. Sci.*, 2018, **9**, 5679–5687.
28 M. Ottonelli, M. Piccardo, D. Duce, S. Thea and G. Dellepiane, *J. Phys. Chem. A*, 2012, **116**, 611–630.
29 R. Liu, H. Ran, Z. Zhao, X. L. Yang, J. L. Zhang, L. J. Chen, H. M. Sun and J.-Y. Hu, *ACS Omega*, 2018, **3**, 5866–5875.
30 C.-Z. Wang, X. Feng, Z. Kowser, C. Wu, T. Akther, M.R.J. Elsegood, C. Redshaw, T. Yamato, *Dyes Pigm.*, 2018, **153**, 125–131.
31 M. J. Kim, M. Ahn and K. R. Wee, *Mater. Adv.*, 2021, **2**, 5371–5380.
32 R. Kurata, A. Ito, M. Gon, Tanaka, K. Chujo and Y. Chujo, *J. Org. Chem.*, 2017, **82**, 5111–5121.
33 X. Wang, J. Zhang, X. Mao, Y. Liu, R. Li, J. Bai, J. Zhang, C. Redshaw, X. Feng and B. Z. Tang, *J. Org. Chem.*, 2022, **87**, 13, 8503–8514.
34 Y. Niko, S. Sasaki, K. Narushima, D. K. Sharma, M. Vacha and G. Konishi, *J. Org. Chem.*, 2015, **80**, 10794–10805.
35 C.-Z. Wang, Z.-J. Pang, Z.-D. Yu, Z.-X. Zeng, W.-X. Zhao, Z.-Y Zhou, C. Redshaw and T. Yamato, *Tetrahedron*, 2021, **78**, 131828.
36 Z.-D. Yu, X.-X. Dong, J.-Y. Cao, W.-X. Zhao, G.-H. Bi, C.-Z. Wang, T. Zhang, S. Rahman, P. E. Georghiou, J.-B. Lin and T. Yamato, *J. Mater. Chem. C*, 2022, (Doi: 10.1039/D2TC01684B)
37 C.-Z. Wang, Z.-D. Yu, W.-X. Zhao, K. Yang, Y. Noda, Y. Zhao, X. Feng, M. R.-J. Elsegood, S. J. Teat, C. Redshaw and T. Yamato, *Dyes Pigm.*, 2021, **192**, 109452.
38 C.-Z. Wang, H. Ichiyanagi, K. Sakaguchi, X. Feng, M. R.-J. Elsegood, C. Redshaw and T. Yamato, *J. Org. Chem.*, 2017, **82**, 7176–7182.
39 C.-Z. Wang, R. Y. Zhang, K. Sakaguchi, X. Feng, X. Q. Yu, M. R.-J. Elsegood, S. J. Teat, C. Redshaw and T. Yamato, *ChemPhotoChem*, 2018, **2**, 749–756.
40 J. Yang, M. Fang and Z. Li, *Aggregate*, 2020, **1**, 6–18.
41 Md. M. Islam, Zhen Hu, Qingsong Wang, C. Redshaw and X. Feng, *Mater. Chem. Front.*, 2019, **3**, 762–781.
42 F. Khan, A. Ekbote, G. Singh and R. Misra, *J. Mater. Chem. C*, 2022, **10**, 5024–5064.
43 S. Grimme, J. Antony, S. Ehrlich and H. Krieg, J. Chem. Phys., 2010, **132**, 154104.
44 J. Liu, Y. Zhang, K. Zhang, J. Fan, C.-K. Wang and L. Lin, Org. Electron., 2019, **71**, 212–219.